

# Theoretical Background

## Water Vapor Sorption Isotherms

The term *sorption* is generally used to describe the initial penetration and the dispersal of the permeant molecules into food matrices (Chirife and Iglesias 1978) and, more generally, into all kinds of polymers (Naylor 1989; Tsujita 1992). This term includes adsorption, absorption into microvoids, and cluster formation. When a food matrix is placed in a humid atmosphere, the relationship between the ambient water activity ( $a_w$ ) and the water concentration ( $Q_w$ ) in the material at a given temperature is described by an equilibrium sorption isotherm ( $Q_w = f(a_w)$ ). Water concentration ( $Q_w$ ) can be defined as the ratio of the mass of sorbed water at equilibrium ( $M_w$ ) to the mass of dry matter ( $M_d$ ):

$$Q_w = \frac{M_w}{M_d} \quad (1)$$

The water activity  $a_w$  at a given temperature can be defined as the ratio of the water vapor pressure ( $p_w$ ) to the saturated water vapor pressure ( $p_{w,0}$ ):

$$a_w = \frac{p_w}{p_{w,0}} \quad (2)$$

Water sorption models are mathematical equations (linking  $Q_w$  and  $a_w$  or  $Q_w$  and  $p_w$ ) used for the prediction of the sorption properties of materials and for analyzing sorption mechanisms and possible interactions between the substrate and water. In some cases, the parameters involved in these equations have physical meaning and can provide useful information on the possible interactions between the product and water (e.g., the dimensionless solvent-polymer interaction parameter  $\chi$  in the Flory–Huggins theory) or on the physical state of the substrate (e.g., amorphous, crystalline, etc.).

## ***Measurement of Water Sorption Isotherms***

The measurement of water sorption isotherms requires bringing the material to an equilibrium state corresponding to a point on the sorption curve and measuring its moisture content when  $a_w$  is fixed or, conversely, measuring an  $a_w$  when moisture content is controlled (Bell and Labuza 2000). In both cases, the method involves changing the total amount of water in the product being studied by imposing a moisture transfer between the air surrounding the product and the product itself. Once equilibrium is reached, the  $a_w$  or the moisture content can be measured using manometric, hygrometric, or gravimetric methods. Manometric methods measure the vapor pressure of water ( $p_w$ ) in equilibrium with the food material by using sensitive manometers. Hygrometric methods measure the equilibrium *relative humidity* (RH) of air in contact with the food material by using dew point or electric hygrometers. Gravimetric methods involve the registration of sample weight changes. The most common technique, recommended by the European COST action 90 on physical properties of foodstuffs, uses thermostated jars filled with saturated salt solutions to set the air RH. The evolution of weight of the sample with time is recorded until the equilibrium is reached (Lomauro et al. 1985a, b).

Hydrous equilibrium is reached very slowly when water activity is high (Timmermann and Chirife 1991; Vos and Labuza 1974). This slowness favors microbiological and biochemical changes in the product that can lead to the generation of small solutes with high water-binding capacity and disturb hydrous equilibrium. To avoid microbial growth, sodium azide, phenyl mercury acetate, or thymol can be added at low concentrations (about 0.05 % of weight), but the consequences on the product and, thus, water binding, are difficult to assess. In addition to these problems of equilibrium time, the detection of the hydrous equilibrium point can be difficult, since many products exhibit two states of equilibrium for the same water content (the so-called hysteresis phenomenon; Simatos 2002). To avoid these two major problems and, particularly, too long an equilibrium time, alternative methods have been developed.

In the last decade, the water sorption of food products has been evaluated using controlled atmosphere microbalance and dynamic automated sorption methods (Fig. 1). The small size of samples and the dynamic airflow around the samples enables the generation of a complete isotherm (from 0 to 95 % RH) in less than a week. Several works using controlled atmosphere microbalance have been published for sorption isotherm measurement in cereal-based products, such as sponge cake (Guillard et al. 2003a; Roca et al. 2008), dry biscuit (Guillard et al. 2004b), or wafer (Bourlieu et al. 2006), and dense materials, such as lipid-based edible films (Bourlieu et al. 2006, 2008, 2009a, 2010) or wheat gluten materials (Angellier-Coussy et al. 2011). Another advantage of this technique is that the mass change kinetics is recorded as a function of time for each water activity tested and permits identifying some water vapor diffusivity in the material (see the section below on water diffusivity and the work of Guillard et al. 2003c). A drawback of the technique is in determining precisely the equilibrium at a given  $a_w$  value for highly

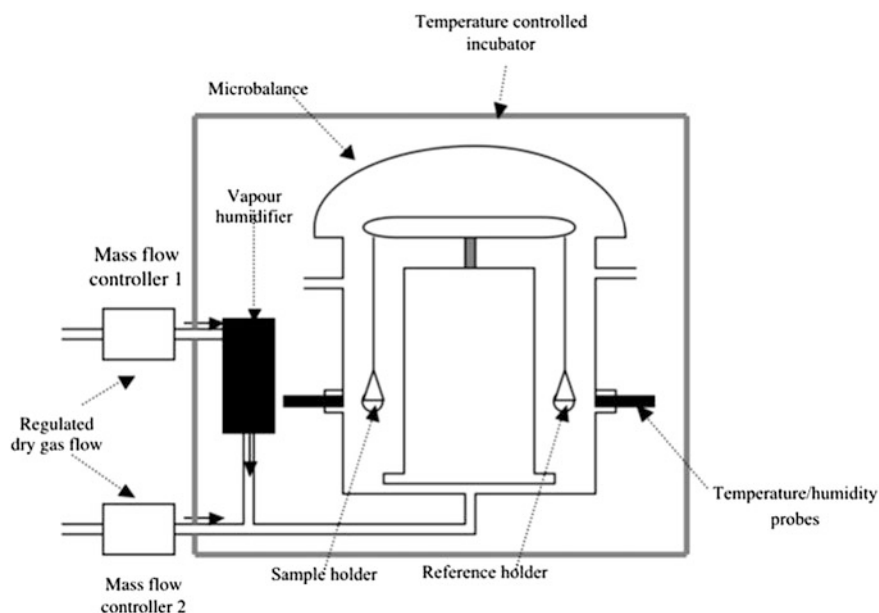


**Fig. 1** Example of sorption balance inspired from the Dynamic Vapor Sorption system of Surface Measurement Systems (Alpertown, Middlesex, UK)

hydrophobic material that sorbs very low amount of water (lower than the sensitivity of the balance). In this case, the length of the step of equilibration at a given humidity should not be automatically finished when the variation in sample mass is lower than a given value (generally  $\pm 0.001$ – $0.002$  % total weight/min). This mass criterion is replaced by a forced length of equilibration, which can vary between 8 h below 60 % RH and reach 24 h above this value for very hydrophobic materials (Bourlieu et al. 2006).

Whatever the matrix, in order to gain more precision of the water sorption at very high water activity ( $>0.95$ ), which is difficult in practice, Baucour and Daudin (2000) have developed a new method whose principle is described in Fig. 2. The apparatus is composed of a set of 10 thermostated cells in which the samples are placed. By using initially saturated air at a given temperature in the first cell and by making successive water vapor pressure drops from cell to cell, a specific range of air RH can be covered (ranging from 98 to 88 % RH over the 10 cells). The principle of this technique is based on the fact that an isothermal pressure drop of 1,000 Pa in an initially saturated air at atmospheric pressure lowers its RH to 99 %, while a variation of  $10^4$  Pa will cause only a negligible change in  $a_w$  of the product, showing that modulation of atmospheric pressure is a much more precise way of adjusting a set of high RH levels. Contrary to saturated salt solutions, this pressure regulation allows the realization of a sequence of RH drops of very low amplitude (1 %) and of high accuracy. Moreover, thin slices of material are submitted to an air flow of very high velocity ( $>10$  m/s), which allows a significantly reduction in the

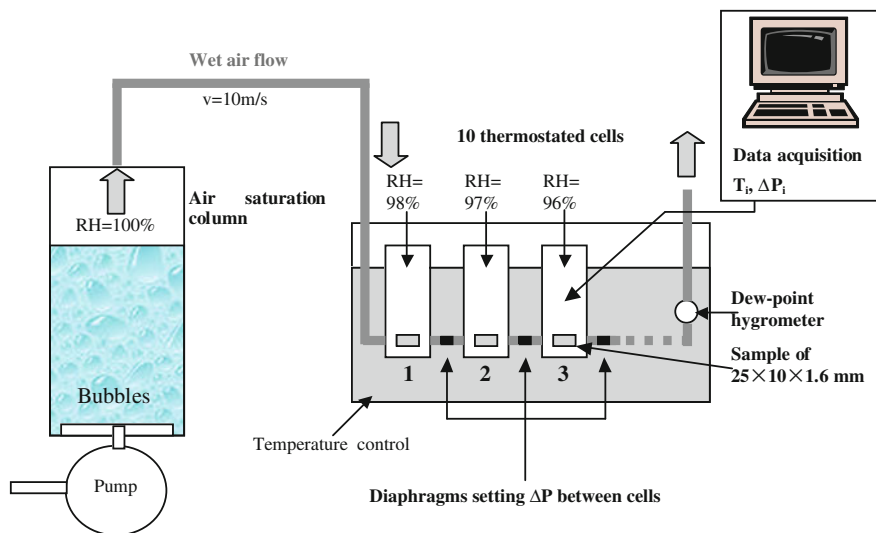


**Fig. 2** Schematic diagram of the experimental apparatus for fast measurement of sorption isotherms developed by Baucour and Daudin (2000).  $T_i$  = temperature in each cell,  $\Delta P_i$  = pressure difference in each cell,  $v$  = wet air flow velocity. Adapted from Baucour and Daudin (2000)

equilibrium time. Baucour and Daudin successfully validated their method with gelatine gel samples, by comparison with the standard saturated salt method. However, this method was not applied to very hydrophobic materials.

### ***Mathematical Description of Water Sorption Isotherm***

Water vapor sorption isotherm in food is first obtained under the form of sets of experimental data. Many different models have been reported for the analysis of sorption of water in various food and nonfood materials (Park 1986; Khalfauoui et al. 2003). For example, in the case of nonedible matrices such as polymers, the classification of Rogers (1965) highlights five fundamental sorption modes: Henry, Langmuir, dual mode, Flory–Huggins, and type IV; the latter has a sigmoid shape and reflects a complex combination of several sorption modes (Fig. 3) (Rogers 1965; Tien 1994). Most food matrices present the Flory–Huggins or type IV shape of isotherms. The type IV is specifically representative of matrices rich in hydrophilic macromolecules, such as cereal-based products. This specific classification, developed for water sorption in polymers, joins that of Brunauer et al. (1940), who first proposed a systematic attempt to interpret adsorption isotherms for any kinds of gas–solid equilibria. Brunauer et al. (1940) classified isotherms into five types (from type I to type V). Type I isotherms characterize microporous

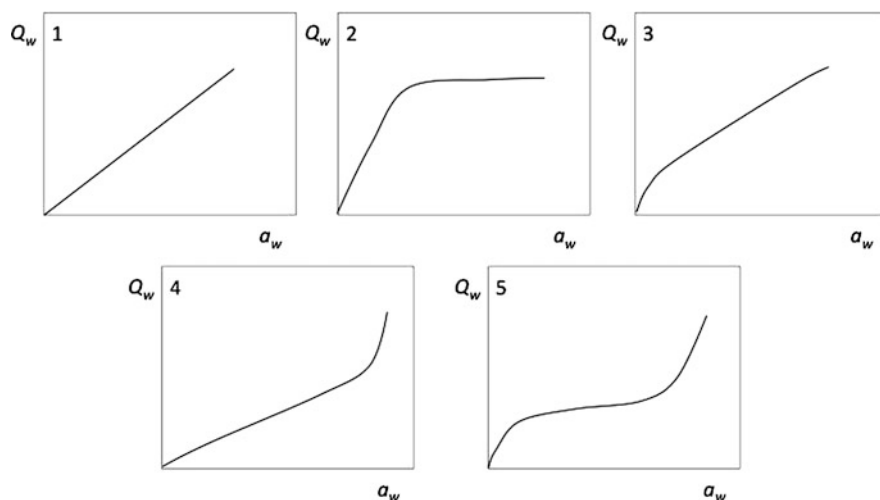


**Fig. 3** Schematic presentation of the types of gas and vapor sorption in the polymer according to the classification of Rogers (1965): (1) Henry's law; (2) Langmuir; (3) Dual-mode; (4) Flory–Huggins; (5) type IV

adsorbents (Langmuir mode). Types II and III describe adsorption on macroporous adsorbents with strong and weak adsorbate–adsorbent interactions, respectively. Types IV and V represent adsorption isotherms with hysteresis.

Water sorption isotherm data are almost always fitted with one or more of a host of theoretical and empirical models (Table 1). No single equation has been found to depict accurately the sorption isotherms of all types of foods in the entire range of water activity. As a consequence, isotherm data are studied individually, and the model that fits and describes most accurately the experimental data is used. Table 1 reports the main equations currently encountered in the modeling of moisture sorption isotherms in food science and their range of validity.

Several common mathematical models for predicting water sorption in food and in nonfood materials are based on the multilayer sorption theory of small molecules onto solid surfaces. These multilayer sorption models combine two modes of sorption. The first sorption mode comprises the formation of a monolayer of sorbate molecules on the surface of the sorbent. The second sorption mode is the multilayer condensation of the sorbate onto the sorbate monolayer, whereby the properties approach those of the pure liquid. The best known example of such multilayer sorption isotherm models is the BET (Brunauer et al. 1938; De Boer 1953) equation in which the multilayer condensation is combined with the Langmuir sorption model for the formation of the monolayer (Table 1).

Whereas the physical interpretation of surface sorption onto rigid adsorbents following the BET equation is rather clear (Adamson 1967), the interpretation of the sorption of water by biopolymer matrices is less evident, since for these systems, the surface adsorption of water is much smaller than the absorption of

**Table 1** Examples of equations used in the modeling of food water sorption isotherms

Reference	Equation <sup>a</sup>	Unknown adjustable parameters	$a_w$ range of validity
Brunauer et al. (1938)	$Q_w = \frac{Q_{\text{mono}} C a_w}{(1-a_w)(1-a_w+Ca_w)}$	$Q_{\text{mono}}, C$	0.3–0.4
Oswin (1946)	$Q_w = c_1 \left( \frac{a_w}{1-a_w} \right)^{c_2}$	$c_1, c_2$	0.3–0.5
Smith (1947)	$Q_w = c_1 - c_2 \ln(1 - a_w)$	$c_1, c_2$	0.3–0.5
Halsey (1948)	$Q_w = \left( \frac{c_2}{\ln a_w} \right)^{-1/c_1}$	$c_1, c_2$	0.1–0.8
Anderson (1946) De Boer (1953) Guggenheim (1966)	$Q_w = \frac{Q_{\text{mono}} C K a_w}{(1-Ka_w)(1-Ka_w+CKa_w)}$	$Q_{\text{mono}}, C, K$	<0.94
Chirife et al. (1983) Ferro Fontan et al. (1982)	$Q_w = \left[ \ln \left( \frac{a}{a_w} \right) \frac{1}{b} \right]^c$	a, b, c	>0.85
Timmerman and Chirife (1991)	$Q_w = \frac{CKQ_{\text{mono}}a_wH'(h)H(h)}{(1-Ka_w)(1-Ka_w+CH(h)Ka_w)}$	$Q_{\text{mono}}, C, K, h$	0–1
Peleg (1993)	$Q_w = k_1 a_w^{n_1} + k_2 a_w^{n_2}$	$k_1, k_2, n_1, n_2$	
Viollaz and Rovedo (1999)	$Q_w = \frac{CKQ_{\text{mono}}a_w}{(1-ka_w)(1-ka_w+CKa_w)} + \frac{Ckk_2a_w^2}{(1-ka_w)(1-a_w)}$	$Q_{\text{mono}}, C, K, k, k_2$	0–1

<sup>a</sup> Nomenclature $Q_w$  moisture content in g/g (dry basis) $Q_{\text{mono}}$  moisture content at the monolayer value g/g (dry basis) $C$  energy constant $K$  additional parameter to the BET equation $H$  and  $H'$  additional functions containing a 4th parameter (h) to the GAB equation $k_1, k_2$  constants in Peleg equation

a, b, c constants

 $n_1 > 1, n_2 > 1$ 

water by the bulk of the material, even at low water contents. In addition, the BET equation fails to take into account the glass transition of the matrix and the molecular interactions of macromolecules and water in the rubbery state.

Experience has shown that the BET equation usually fits poorly the water sorption by biopolymer matrices at high water activities ( $a_w > 0.4$ ). For this reason, the so-called Guggenheim–Anderson–de Boer (GAB) isotherm equation was introduced and is often applied to fit and analyze water vapor sorption by biopolymer matrices (Anderson 1946; Roos 1995). The GAB equation is obtained from the BET equation by transformation of the water activity axis:

$$a_w \rightarrow Ka'_w \quad (3)$$

Then,

$$Q_w = \frac{Q_{\text{mono}} C K a'_w}{(1 - Ka'_w)(1 - Ka'_w + CKa'_w)} \quad (4)$$

It should be noted that the physical significance of the GAB equation for the sorption of water by biopolymer matrices is even more limited than that of the BET equation, because of its unphysical divergence at water activity values below unity for values of  $K$  larger than 1. Indeed, whereas the BET equation diverges as  $(1 - a_w)^{-1}$  for  $a_w \rightarrow 1$ , the GAB equation diverges at a critical water activity  $a_w = K^{-1}$ . This unphysical divergence was observed, for example, for the GAB fit of all maltopolymer-maltose samples studied in the work of Ubbink et al. (2007).

$Q_{\text{mono}}$  is usually interpreted as the water content at which a full monolayer of sorbate coverage is reached, and in the relevant limit of  $C \gg 1$ ,  $C$  determines the steepness of the initial rise to the monolayer plateau and is thus related to the free energy of sorption at low partial pressures. It was hypothesized that both parameters are thus related to the glassy-state properties of the matrices (Ubbink et al. 2007). In contrast, as was suggested by Ubbink et al (2007),  $K$  should be related either to the rubbery-state properties or to the glass transition of the matrices, since  $K^{-1}$  equals the water activity at which the GAB equation diverges.

The GAB equation was found to represent adequately the experimental sorption data in many foodstuffs, such as amorphous maltodextrin–glycerol matrices (Roussanova et al. 2010), carbohydrate mixtures (Ubbink et al. 2007), dried fruits (Maroulis et al. 1988), tapioca (Sanni et al. 1997), cookies and corn snacks (Palou et al. 1997), and hydrophobic films (Bourlieu et al. 2006, 2009). However, in the very high  $a_w$  range ( $a_w > 0.94$ ), which is of most interest for fresh foods, the GAB equation failed to describe the water vapor sorption. Alternative empirical models, such as the Peleg (1993) or the Ferro-Fontan equations (Ferro-Fontan et al. 1982; Chirife et al. 1983) were consequently proposed and were found adequate to predict moisture content in the very high  $a_w$  range in products such as gelatine gel (Baucour and Daudin 2000) or sponge cake (Guillard et al. 2003a).

## Water Sorption Behavior in Foodstuffs

The equilibrium moisture sorption isotherms of hydrophilic food products usually show a large degree of upturn at high activities. Two phenomena are suggested for interpretation of the equilibrium isotherm upturn in dense materials: (1) plasticization of the material by water (when the product, initially in a glassy state, passes through its glass transition and reaches the rubbery state) and/or (2) clustering of water molecules. An in-depth analysis of water sorption isotherms allows analyzing this phenomenon of water clustering, as described below.

Water molecules have a tendency to form clusters when absorbed in a polymer. To provide a measure for clustering, Zimm and Lundberg (1956) defined the clustering integral  $G_{w,w}$ . The ratio of the clustering integral to the partial molecular volume,  $G_{w,w}/V_w$ , called the *clustering function*, is obtained from the equilibrium data:

$$\frac{G_{w,w}}{V_w} = -(1 - \phi_w) \left[ \frac{\partial(a_w/\phi_w)}{\partial a_w} \right]_{P,T} - 1 \quad (5)$$

where  $v_w$  is the partial molecular volume for water. Positive values of the clustering function indicate that water in the polymer matrix forms small clusters, or “pockets,” between the polymer chains. Conversely, negative values of the clustering function indicate that water is molecularly dispersed in the polymer matrix. The state  $G_{w,w}/v_w = -1$  represents a random distribution of noninteracting water molecules. The quantity  $\phi_w G_{w,w}/v_w$  has been interpreted as the mean number of solvent molecules in the neighborhood of a given solvent molecule in excess of those provided by the mean solvent concentration. The sum  $(1 + \phi_w G_{w,w}/v_w)$ , therefore, is the mean cluster size.

## Water Diffusion

Moisture transfer in foodstuffs and, more particularly, in multidomain systems occurs because of a difference in water activity between domains, which acts as a driven force for the mass transfer. Moisture gain or loss from one region to another region will continuously occur in order to reach thermodynamic equilibrium between the different domains involved. The movement of water within solids is complex and may be explained by different mechanisms, such as molecular diffusion of liquid water due to concentration gradient, liquid movement due to capillary flow, liquid movement due to gravity, vapor diffusion due to partial vapor pressure, Knudsen diffusion, and surface diffusion (Barbosa-Canovas and Vega-Mercado 1996) (see Fig. 4). In order to explain, describe, and predict moisture movements within solid foods, mathematical models of increasing complexity have been proposed in the literature for decades. In the following section, we will provide an overview of these modeling approaches, discuss their pros and cons, and make conclusions about the most useful ones.

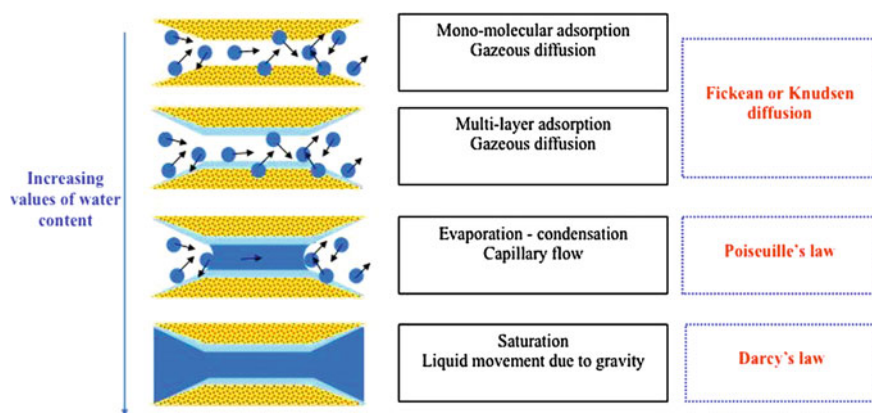


**Fig. 4** Schematic presentation of the mechanisms of water transport in a foodstuff contributing to the overall water movement



## ***Modeling Moisture Transfer***

Modeling moisture transfer within solid food products has been widely studied because it is necessary for the dimensioning of food-processing units such as drying or storage. Models encountered in the literature can be classified as theoretical models, semitheoretical models, phenomenological models, the Stefan–Maxwell approach, and empirical models according to the assumptions made for internal water transport mechanisms. In Table 2, some of the main mathematical theories are presented according to this classification. For a more exhaustive list of mathematical models, see the review of Waananen et al. (1993), who reported the drying theories encountered in the literature from 1907 to 1992.

### **1. Theoretical or Mechanistic Models**

Theoretical models (or mechanistic models) presuppose the knowledge of the mechanisms of water transport involved in the product being studied—that is, the fluxes and the driving forces involved. In order to tentatively explain the contribution of several mechanisms to an overall water movement, a combination of several driving forces could be used. For example, the “Philip and De Vries” or “Berger and Pei” theory combines liquid capillarity and vapor diffusion (Table 2). Thorvaldsson and Janestad (1999) tentatively tried to take into account liquid and vapor water diffusion in their model and developed a model based on Fick’s second law, including two diffusion coefficients for liquid and vapor water, respectively. They successfully validated their model with bread slabs during drying. But in a general manner, such combinations complicate the partial differential equation of diffusion a lot. Difficulty was also encountered in determining separately liquid and water vapor diffusion coefficients. As a result, a simple diffusion model based on Fick’s second law (Eq. 6) is usually preferred by investigators to represent the overall moisture transfer in solid foodstuffs, even though, in this case, Fick’s law is extrapolated out of its application conditions:

$$\frac{\partial Q}{\partial t} = \frac{\partial}{\partial x} D \frac{\partial Q}{\partial x} \quad (6)$$

where  $D$  is the coefficient of diffusion or diffusivity ( $\text{m}^2 \text{s}^{-1}$ ),  $Q$  is the concentration ( $\text{kg m}^{-3}$ ),  $x$  is the distance (m), and  $t$  is time (s).

These theoretical models based on Fick’s second law yield to a good description and prediction of the moisture transfer between the product and the surrounding medium, provided that the assumptions and parameters required in the model formulation were verified and known (sample geometry, moisture diffusivity value, initial and boundary conditions, etc.). Fick’s second law has been extensively and successfully used for describing and predicting various processes, such as, for example, soaking of soybeans (Hsu 1983), drying of corn extruded pasta (Andrieu and Stamatopoulos 1986), moisture distribution in dough/raisin mixtures (Karathanos and Kostaropoulos 1995), dehydration of prune (Sabarez et al. 1997; Sabarez and Price 1999), or drying of cashew kernel (Hebbbar and

**Table 2** Some of the main theories proposed for water transport modeling in food products

Model	Reference	Driving force	Postulated mechanisms	Mass transport equation
Theoretical models	Fick (1855)	$\nabla X_L$	Liquid diffusion	$\frac{\partial X}{\partial t} = \frac{\partial}{\partial x} \left( D_{\text{eff}} \frac{\partial X}{\partial x} \right)$
	Okozuno and Doi (2008)		Liquid diffusion + stress-driven diffusion term	
	Colon and Aviles (1993)	$\nabla P$	Liquid capillarity	$\frac{1}{A} \frac{\partial X}{\partial t} = -K_H \nabla P$
	Philip and De Vries (1957)	$\nabla X_v, \nabla T, \nabla P$	Liquid capillarity + vapour diffusion	$\frac{\partial X}{\partial t} = \nabla \cdot (D_m \nabla X) + \nabla \cdot (K_{rm} \nabla T) + \frac{\partial K_H}{\partial z}$
Semi-theoretical	Berger and Pei (1973)	$\nabla X_L, \nabla X_v$	Liquid capillarity + liquid diffusion + vapour diffusion	$D_L \rho_L \frac{\partial^2 X}{\partial x^2} + D_v \left[ (\varepsilon - X) \left( \frac{\partial^2 \rho_w}{\partial x^2} \right) - \left( \frac{\partial X}{\partial x} \right) \left( \frac{\partial \rho_w}{\partial x} \right) \right]$ $= (\rho_L - \rho_w) \left( \frac{\partial X}{\partial t} \right) + (\varepsilon - X) \left( \frac{\partial \rho_w}{\partial t} \right)$
	Whitaker (1980)	$\nabla X_L, \vec{g}, \nabla X_v, \frac{\nabla P}{\rho}$	Bulk flow	$\frac{\partial (\Psi_\gamma \langle \rho \rangle_\gamma)}{\partial t} + \nabla \cdot (\langle \rho \rangle_\gamma \langle v \rangle_\gamma) + \frac{1}{v} \int \rho_l (v_1 - w) \vec{n}_l dA$ $= \nabla \cdot (\langle \rho \rangle_\gamma \cdot D_{\text{eff},v} \cdot \nabla \langle \rho \rangle_\gamma / \langle \rho \rangle_\gamma)$ $F_s X_{\text{in}} - F_{\text{out}} X_{\text{out}} =$ $d(M_p X_{\text{avg}}) + GF_{\text{sfines}} X_{\text{w fines}} + V(Y_{\text{out}} - T_{\text{in}})$ $\frac{\partial X_v}{\partial t} = \frac{\partial}{\partial x} (D_v \frac{\partial X}{\partial x}) \text{ and } \frac{\partial X}{\partial t} = \frac{\partial}{\partial x} (D_L \frac{\partial X}{\partial x})$ $MR = a \exp(-kt)$
	Thorvaldsson and Janestad (1999)	$\nabla X_v, \nabla X_L$	Liquid diffusion + vapour diffusion	
	Henderson and Pabis (1961)	[—]	Bulk flow	
Phenomenological Stefan-Maxwell	Henderson (1974)	[—]	Bulk flow	$MR = a \exp(-k_1 t) + b \exp(-k_2 t)$
	Bruce (1985)	[—]	Bulk flow	$MR = \exp(-kt)$
	Luikov (1966, 1975)	$\nabla X, \nabla T, \nabla P$	Vapour diffusion, bulk flow, liquid	$\vec{J}_i \sum L_{ik} \vec{X}_i$
	Gekas (1992)	$\nabla X_i$	Bulk flow	$\frac{\Delta x_i}{\bar{x}_i} = \sum_j \frac{\bar{u}_i - \bar{u}_j}{k_{ij}}$
Empirical models	Thompson et al. (1968)	[—]	[—]	$t = a \ln MR + b(\ln MR)^2$
	Wang and Singh (1978)	[—]	[—]	$MR = 1 + at + bt^2$

(continued)

Table 2 (continued)

Nomenclature		
$\langle \rangle$	Average value	$\vec{J}_i$
$\alpha$	The volume fraction of air in the pores	Heat and mass diffusion flux (Luikov's theory)
$\varepsilon$	Void fraction of the solid	Thermodynamic forces giving rise to $\vec{J}_i$ (Luikov's theory)
$\rho$	Density	Exposed area
$\tau$	Factor taking into account the tortuosity	Gas phase effective diffusivity
$v$	Individual mass velocity (Whitaker theory)	Effective diffusivity (Fick's law)
$\Psi$	Volume fraction of the phase	Liquid conductivity
$\nabla$	Gradient	Overall isothermal moisture diffusivity
$a$	Constant	Vapour diffusion coefficient
$b$	Constant	Solids feed
$k_1$	Constant	Dry air stream
$k_2$	Constant	Unsaturated hydraulic conductivity
$k_{ij}$	Mass transfer coefficient	Overall thermal moisture diffusivity
$l$	Evaporating species (Whitaker theory)	Luikov phenomenological coefficient
$\vec{n}$	Unit normal vector	Dry solid holdup in the dryer
$T$	Time	Moisture ratio $(X - X_e/X_0 - X_e)$ with $X_0$ , initial moisture content and $X_e$ , equilibrium moisture content
$u$	Velocity	Pressure
$x$	Spatial dimension	Temperature
$\bar{x}_i$	Arithmetic mean mole fraction of a component i	Dimensionless heat parameter
Subscripts		
$s$	Solid phase	Moisture content in kg of water/kg of dry solids
fin	Particles carried by the air	Air moisture content
$\gamma$	Gas phase	Coordinate where mass transfer occurs
$w$	Vapour phase	

Rastogi 2001). More recently, Fick's second law has been used to describe moisture transfer in cellular solid foods (Voogt et al. 2011) and to describe water migration mechanisms in amorphous powder material and the related agglomeration propensity (Renzetti et al. 2012).

Fick's second law has also been used to predict moisture transfer in more complex systems, such as multidomain food products (or composite foods)—for example, breakfast cereal–raisin mixtures, ready-to-eat sandwiches, cereal-based pastry filled with a savory, moist filling, and so forth—in which moisture transfer occurs from the wet into the dry domain until thermodynamic equilibrium between the food components is reached (Guillard et al. 2003; Bourlieu et al. 2008; Roca et al. 2008). This moisture transfer affects the physical, sensory, and microbial qualities of the food and, especially, leads to the loss of texture for the dry cereal-based compartment in the common case of association of a crispy cereal texture with a moist filling. Modeling moisture transport within these products is of great interest in order to predict water distribution within the product and, thus, its shelf life. In the above-mentioned studies (Guillard et al. 2003; Bourlieu et al. 2008; Roca et al. 2008), Fick's second law succeeded in predicting water distribution in each domain of the composite foods, even in porous products, which were assimilated to continuous matter. Diffusivity was found to vary with moisture content (Guillard et al. 2003), which was successfully taken into account in the model, as well as various interfacial conditions such as nonperfect contact between the domains (Roca et al. 2008) and the presence of an edible barrier film at the interface between the domains (Guillard et al. 2003; Bourlieu et al. 2006). Such mathematical models, even if they did not represent the water transport mechanisms that prevail in the system, can be used as decision-making tools to design composite food with optimized shelf life (e.g., dimensions of the different domains, thickness of the edible barrier film, initial water activity of the wet compartment, etc.) (Roca et al. 2008).

## 2. Semi-theoretical Models

Semi-theoretical models offer a compromise between the theory and its ease of use (Fortes and Okos 1981). They are generally derived by simplifying the general series solution of Fick's second law. They are less time consuming than theoretical models in calculations. They are valid only within the temperature, RH, air flow velocity, and moisture content range for which they were developed, but the key point is that they do not need assumptions on food geometry, mass diffusivity, and conductivity, as compared with theoretical models such as those based on Fick's second law. As is shown in Table 2, semi-theoretical models developed for the drying of thin layers, such as the Henderson and Pabis model or the two-term model, relate moisture ratio of the food being studied to time through an exponential relation. The Henderson and Pabis model is the first term of a general series solution of Fick's second law (Henderson and Pabis 1961). This model was successfully used to model drying of corn (Henderson and Pabis 1961), wheat (Watson and Bhargava 1974), rough rice (Wang and Singh 1978), and mushrooms

(Gürtas 1994). The slope of the Henderson and Pabis model is under conditions related to the water effective diffusivity (Madamba et al. 1996). The two-term model is the first two terms of a general series solution of Fick's second law and has also been used to describe the drying of corn (Henderson 1974; Sharaf-Eldeen et al. 1980) and white beans and soybeans (Hutchinson and Otten 1983). However, it requires a constant product temperature and assumes a constant diffusivity. The Lewis model is a special case of the Henderson and Pabis model and was used to describe the drying of barley (Bruce 1985), wheat (O'Callaghan et al. 1971), and cashew nuts (Chakraverty 1984). These three semitheoretical models have been compared by Ozdemir and Devres (1999) for describing the isothermal roasting of hazelnuts. The two-term model obtained the highest correlation coefficient between experimental and predicted data, followed by the Henderson and Pabis model and, eventually, by the Lewis model. Nowadays, due to higher and higher computer capacities, these simplified models are less used.

### 3. Phenomenological Models

Unlike rigorous theoretical models, phenomenological models offer the possibility of modeling moisture transport phenomena without a priori hypotheses concerning the transport mechanisms that are involved, provided that the driving forces are known. A system under study is treated as a black box, and equations are written connecting the fluxes to the driving forces acting upon the system. Apparently, these equations are very similar to the ones describing rigorous steady-state equations in a Fickian diffusion. The difference in these phenomenological models lies in the fact that phenomenological coefficients are used instead of strict mechanistic coefficients characterizing moisture transport like diffusivities. Models based on irreversible thermodynamics theory belong to the phenomenological models. According to this theory, any flux is given by a linear relationship of all the driving forces of the system. The most common phenomenological model is the Luikov model (Table 2), which takes into account not only moisture and thermal diffusion, but also the cross-effects between thermal and moisture gradients (Soret and Dufour effects). Luikov's (1975) model has been widely used for heat and mass transfer in capillary porous products (Fortes and Okos 1981; Dantas et al. 2003) or in rough rice (Hussain et al. 1973), maize kernels (Neményi et al. 2000), wood and peanut pod (Kulasiri and Samarasinghe 1996). Another phenomenological model is to consider the difference in the chemical potential of water, instead of moisture content, as the driving force in the formulation of Fick's second law. By combining models based on irreversible thermodynamics and Fick's second law expressed with chemical potential, phenomenological coefficients ( $L_{ik}$ ) can be determined.

The Stefan–Maxwell approach for mass transfer is a kind of model combining both a mechanistic and a thermodynamic character. It is thermodynamic in the sense that the chemical potential is used as the driving force. However, it is not a phenomenological model, because friction is assumed to be a transport mechanism. The main idea of the model is that the transport of a component, which is due to its

potential, creates a force that is balanced by the friction with the surroundings. Friction is expressed in terms of velocity differences of a pair of components. Since fluxes are not explicitly treated contrary to Fick's laws, this model was progressively given up by experimentalists. Even so, the simplified version developed by Wesselingh and Krishna (1990), cited in Gekas (1992), transforming differentials in finite differences makes the Stefan–Maxwell approach very interesting. Whereas the Stefan–Maxwell approach is successfully used in material science for describing water transport, for example, through hydrogel (Hoch et al. 2003) or zeolite membranes (Gardner et al. 2002), it is rarely used in food science.

#### 4. Empirical Models

Empirical models derive from a direct relationship between average moisture content and time. They are very useful if neither the mechanisms nor the fluxes or driving forces are identified clearly in a transport problem, which is easily the case in very complex systems. In general, the aim of such models is to establish a relationship between a dependent variable and a number of independent variables. They do not provide any information on the mechanisms occurring during the process, although they succeed in describing the moisture content evolution for the conditions of the experiment. Empirical models have been extensively used for describing the drying curve of various foodstuffs, especially when drying conditions are not well characterized or constant throughout the experiment. Examples of such models are the *Thompson* model and the *Wang and Singh* model (Table 2). The *Thompson* model was used to describe shelled corn drying for temperatures between 60° and 149 °C (Thompson et al. 1968), and the *Wang and Singh* model was used to describe drying of rough rice (Wang and Singh 1978). Because knowledge has considerably improved for knowing and controlling conditions of transfer (e.g., temperature, boundary conditions, etc.) in food processing, mechanistic approaches could now be used most of the time, and therefore, such empirical models have been given up.

In conclusion, the overall water transport in foods products is complex and results from different mechanisms, which cannot be easily distinguished. Molecular diffusion according to Fick's law is generally assessed as the main water transport mechanisms in food matrices (Eq. 6). The moisture diffusivity ( $D$ ) in the foodstuff is, consequently, an apparent or effective diffusivity ( $D_{\text{eff}}$ ) representative of the overall moisture transport. Even though this method is not perfectly sound theoretically, because Fick's law is extrapolated out of its application conditions, it is a very convenient and numerically accurate approach to describing moisture content transport during processing and storage, provided that effective diffusivity ( $D_{\text{eff}}$ ) is well determined, as well as boundary conditions.

## ***Determination of Water Diffusivity in Solid Products***

To obtain an estimate of the water effective diffusivity for a given material in well-defined environmental conditions, two choices exist: (1) obtain values from the literature for the same or similar products or (2) measure these values. As regards water and solutes, ( $D_{\text{eff}}$ ) databases exist, such as, for example, the one reported by Doulia et al. (2000). Nevertheless, the large variety of foodstuffs is not entirely represented in such databases, and, for a given material, ( $D_{\text{eff}}$ ) is calculated in restrictive conditions of temperature and humidity range. In most cases, ( $D_{\text{eff}}$ ) values cannot be extrapolated to different materials or in different conditions of temperature and humidity. Consequently, direct measurements of ( $D_{\text{eff}}$ ) should be performed to determine precisely the moisture transport of the food.

Unfortunately, there is no standard method of diffusivity estimation. Contrary to water sorption isotherm, moisture diffusivity cannot be directly measured from experiments. Moisture transfer must be generated in the product under study and then monitored as a function of time and/or position in the food. Then experimental kinetics (e.g., average moisture content evolution with time or, for a given time, local water distribution as a function of position) must be fitted using a mathematical model (analytical or numerical solution of Fick's second law) in order to identify the diffusivity by using an optimization procedure. One of the common criteria used for optimization is the minimizing of the sum of squared error between experimental values and those predicted by the model.

### **a. Solving Fick's Second Law**

In many cases, Fick's second law can be analytically solved if several assumptions are experimentally verified, such as, for example, uniform initial concentration, plane sheet or spherical geometry, monodirectional transfer, no external resistance to mass transfer (especially in the case of transfer between food and surrounding atmosphere), no shrinkage or swelling, and constant ( $D_{\text{eff}}$ ). Such analytical solutions covering varying specimen geometry are found in the famous book of Crank (1975).

Unsteady mass transfer problems can also be solved numerically by transforming the partial differential equation of mass transfer into finite-difference equations in both space and time domains (Burden and Faires 1997). An advantage of such numerical solutions is that nonlinear terms of the partial differential equation can be solved covering presence of more complex initial and boundary conditions than with analytical solutions, including external mass transfer resistance, simultaneous mass transfer and chemical reaction, moving boundaries, and so forth. ( $D_{\text{eff}}$ ) dependence on temperature and moisture content can also be taken into account through various multiparameter equations. Different schemes of discretization exist, such as the Crank–Nicolson one. Nowadays, due to the use of ODE solvers integrated in most commercial software (see, e.g., ode15 s or ode45 functions of MATLAB<sup>®</sup> software), only the spatial second-order derivatives in Eq. 6 are discretized using, for example, a three-point central difference formula.

Then the discretized form of Eq. 6 and its boundary and initial conditions is solved using an ODE routine that adjusts the size of the step of time for calculations according to the importance of moisture content variations. Such ODE solvers facilitate the solving of Fick's second-law-based system a lot and permit routine consideration of more complex assumptions for mass transfer (e.g., swelling or shrinkage of the product, diffusivity variations as a function of moisture content, etc.).

Both analytical and numerical solutions perform simulations of local moisture content in time and space domains in the food, which can allow calculation of the average moisture content evolution with time of the product being studied.

#### b. Identification of Diffusivity

Once a mathematical model simulating moisture transfer in the experiment is set up, diffusivity values or parameters of diffusivity law must be identified by comparison with experimental data. Either local or global moisture content evolution with time can yield an effective diffusivity or parameters of diffusivity law by using an optimization procedure. The most used criterion for optimization is the minimizing of root mean squared error between experimental and predicted data (Gill et al. 1981).

A variety of experiments are designed to suit the particular needs of the analytical or numerical solution chosen, including permeation methods, sorption or drying kinetics, and moisture distribution profiles. A detailed description of some of these methods was given by Zogzas et al. (1994) and is completed in the following paragraphs.

#### c. Experimental Setups for Diffusivity Determination

##### i. Permeation Methods

These methods were primarily developed for the evaluation of moisture diffusion through polymer membranes.

*Steady state.* A thin sheet of material is placed between two sources maintained at a constant concentration of diffusant (e.g., between two compartments that are maintained at different isothermal RH by means of a suitable buffer or saturated salt solutions). After a time period, the surfaces of the sheet come into equilibrium with the diffusant sources, thus developing a constant gradient of surface concentrations, leading to steady state conditions of diffusion. This state can be expressed, for a plane sheet, by the following equation:

$$J = D_{\text{eff}} \frac{(C_1 - C_2)}{L} \quad (7)$$

where  $C_1$  and  $C_2$  are concentrations ( $\text{kg m}^{-3}$ ) in diffusing substance at each side of the layer and  $L$  is the thickness of the layer (m).

Diffusivity can be estimated by measuring the flux of the diffusant, with known surface concentrations and thickness of the material sheet, which can be done experimentally by successive weighing of the diffusion cells at different time



intervals. Varzakas et al. (1999), Floros and Chinnan (1989), and Djelveh et al. (1988, 1989) successfully used this method for determining  $D_{\text{eff}}$  values of enzymes in polysulphone membranes, hydroxyl (OH<sup>-</sup>) through tomato skin, and NaCl through gels and meat products, respectively. This method was often applied to edible coatings (ethyl cellulose, zein, wheat gluten, etc.) (Bourlieu et al. 2009).

*Time-lag method.* This method is based on the time period prior to the establishment of the steady state diffusion. If, by some convenient means, one of the sheet surfaces is maintained at  $C_1$  concentration while the other is maintained at zero concentration, after a theoretically infinite time period, a steady state condition of diffusion will be achieved. Assuming that the diffusivity is constant, that the sheet is initially completely free of diffusant, and that the diffusant is continually removed from the low-concentration side, the amount of diffusant that will permeate the sheet, when  $t \rightarrow +\infty$ , is given as a linear function of time by Eq. 8:

$$W_t = \frac{D_{\text{eff}} C_1}{L} \left( t - \frac{L^2}{6D_{\text{eff}}} \right) \quad (8)$$

where  $W_t$  is the amount of diffusant ( $\text{kg m}^{-2}$ ).

By plotting  $W_t$  against time, after a relatively large time interval, a straight line results, intercepting the  $t$ -axis at the quantity ( $L^2/6D_{\text{eff}}$ ). From this intercept,  $D_{\text{eff}}$  may be deduced.

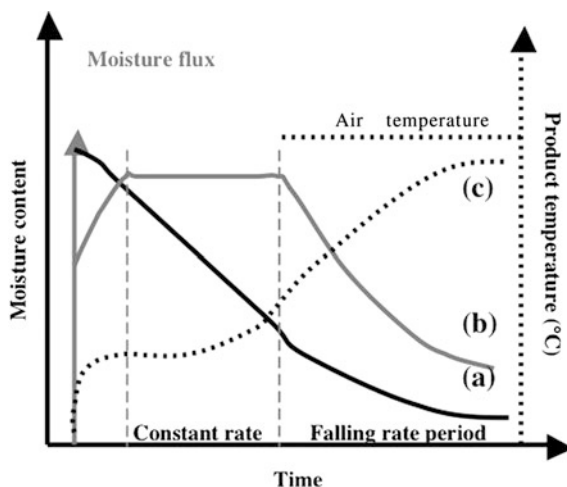
Although these two permeation methods seem to be simple in application, they raise experimental problems, including the difficulties of manufacturing a thin material sheet of constant thickness and homogeneous structure, the erroneous measurement of the flow rate of diffusion, and the swelling of the membrane material under experimental conditions. Therefore, this methodology is essentially used for the thin membranes of materials such as packaging film.

## ii. Water Sorption or Desorption (Drying) Kinetics

During drying or desorption experiments, a geometrically defined sample (e.g., a slab of  $L$  thickness) is dried in a renewed air flow under conditions in which the partial pressure of water and temperature in the air are kept constant. Under these conditions, after an initial, very short period (constant rate period) during which the rate of drying is constant, there follows a so-called *falling rate period* (Fig. 5), in which the rate is assumed to be controlled by internal mass transfer resistance—that is, by the moisture diffusivity within the material. The weight loss or gain with time of the foodstuff is monitored. The usual practice has been to assume that the effective diffusion coefficient is indeed constant over the entire falling rate period or, at least, over significant portions of this period. Consequently, the simplified analytical solution of Fick's second law (Eq. 9) can be applied for modeling moisture transfer in a slab:

$$\frac{X - X_e}{X_0 - X_e} = \frac{8}{\pi^2} \exp \left[ -\frac{\pi^2 D_{\text{eff}}}{4 L^2} t \right] \quad (9)$$

**Fig. 5** Typical drying curve with (a) moisture content evolution in the product, (b) drying kinetic and (c) temperature evolution in the product (from Daudin 1983)



where  $X_e$  is the moisture content ( $\text{kg m}^{-3}$ ) of the product in equilibrium with RH in the air,  $X_0$  is the initial moisture content ( $\text{kg m}^{-3}$ ), and  $L$  is a characteristic dimension (m) (e.g., slab thickness).

The drying process can then be represented by one or more straight lines, when the quantity  $\text{Log}(X - X_e/X_0 - X_e)$  is plotted against time. Obviously, this method is simple and has often been used for moisture diffusivity determination—for example, by Biquet and Guilbert (1986) in agar gels, by Hebbar and Rastogi (2001) in cashew kernel, by Lazarides et al. (1997) in fruit and vegetables tissues undergoing osmotic processing, by Raghavan et al. (1995) in raisins, and so forth. However, in Eq. 9, several assumptions are made, such as constant diffusivity, surface area, and slab thickness, but also negligible external mass transfer resistance between air and sample. In reality, a modification of surface area due to swelling, shrinkage, or porosity changes can occur in the food. Shrinkage can be monitored, and a corrected geometry must be used in the calculations. However, diffusivity dependence on moisture content cannot be represented using Eq. 9. More appropriate alternative solutions of Fick's second law (numerical solution) taking into account possible change in the dimensions of the sample, as well as the particular boundary conditions and the diffusivity dependence on moisture content and/or temperature, have thus been proposed and used. For example, Bonazzi et al. (1997) developed a conventional diffusive model with variable diffusion coefficient, solved by finite difference calculations in a solid-related frame of coordinates, in order to identify moisture diffusivity in gelatine slabs during drying. More recently, Batista et al. (2007) also used a numerical scheme to obtain a diffusivity law in thin chitosan layer, taking into account shrinkage. Such numerical solutions are nowadays currently used in the field of drying technology, and a list of examples could not be exhaustive.

Moisture changes in a foodstuff can also be measured in adsorption type under controlled conditions of RH. The mass evolution with time is monitored up to

equilibrium. Time before reaching equilibrium varies as a function of sample geometries. The thinner the sample, the more rapidly the equilibrium will be achieved. Biquet and Labuza (1988) and Leslie et al. (1991) utilized this method with chocolate films and starch gels, respectively. The simplest way to control RH is to put the sample over saturated salt solutions (Labuza et al. 1976). The main advantage of this method lies in the less severe conditions imposed on the product, as compared with a conventional drying technique. As a consequence, the sample is subjected less to collapse or shrinkage. However, this methodology is time consuming (several days or even weeks before obtaining equilibrium). Consequently, as was explained above for the measurement of water sorption isotherms, microbial development can occur on the surface sample at high RH level and necessitate adding some antimicrobial additives.

Recently, the use of Cahn microbalance (or other, similar systems) to measure water vapor sorption kinetic in a thin piece of material (<30 mg) has permitted significantly reducing the time before equilibrium is reached and improving the study of water diffusivity in food and nonfood materials (Guillard et al. 2003c; Bourlieu et al. 2006; Oliver and Meinders 2011). The Cahn balance allows one to obtain a complete water adsorption or desorption kinetic for several successive RH levels in less than 4 days (depending on the material and temperature). From the transient state data obtained for each RH step studied, a diffusivity value can be identified. This methodology has the advantage of permitting one to observe diffusivity variations as a function of moisture content in the product without making assumptions a priori on the diffusivity law.

A significant problem is often encountered during both drying and sorption kinetics measurement by the formation of a boundary layer, offering a considerable external resistance to moisture transfer. This problem is faced again by stirring the surrounding fluids. However, stirring has proven inadequate, especially in cases where the internal resistance to mass diffusion is small enough. In that case,  $D_{\text{eff}}$  values characterize an overall mass transport representing both the internal diffusion and the external mass transfer at the interface. Since external resistance to mass transfer is difficult to determine experimentally, numerical solutions that take into account both the internal diffusion and the mass transfer coefficient at the interface can scarcely be applied for diffusivity identification. Nevertheless, in order to improve the accuracy of their moisture diffusivity values identified from water sorption kinetics measured in a Cahn microbalance, Roca et al. (2008) have determined the external mass transfer coefficient dependent of the geometrical and air flow characteristics encountered in the microbalance used by these authors (DVS from SMS, London) and routinely used this correction when identifying their diffusivity values.

### iii. *Moisture Local Distribution Profiles*

In this method, the local concentration of the diffusant within the sample as a function of distance is determined for the case of one-dimensional diffusion. One of the best ways to determine the concentration distance profiles is by using a long cylindrical sample undergoing one-dimensional diffusion along its axis, in a

sorption process. After a specified time interval, the cylinder is sliced in many equal parts, and the moisture content of each slice is gravimetrically or chemically analyzed. Another technique is to use two cylindrical samples of the same radius but different in diffusant concentration (Fig. 6). At time  $t = 0$ , the two cylinders are joined together, and after a specified time interval, the diffusant concentration profile along the axis can be determined by slicing and weighing the samples slices. Diffusivity is then evaluated by identification from the experimental distribution profiles, using either an analytical or a numerical solution of Fick's second law with appropriate boundary conditions.

Contrary to sorption or drying kinetics, where the global loss or gain of moisture as a function of time is measured, the moisture distribution profile method directly provides spatial information about moisture diffusion, which can be compared with the local moisture contents predicted by the model. That means that diffusivity can be identified from a set of data obtained for only one diffusion time. Therefore, the diffusivity can be obtained more rapidly with a local distribution profile than with a global profile, provided that diffusivity is high enough to permit detection and quantification of water content in a thin slab of material.

Warin et al. (1997), Motarjemi (1988), Karathanos and Kostaropoulos (1995), and Litchfield and Okos (1992) have successfully used this method for measuring sucrose diffusivity within agar gels, moisture distribution profiles in meat, moisture distribution in dough/raisin systems, and water diffusivity in spaghetti, respectively. Recently, this approach was revisited by Guillard et al. (2003a) to identify moisture diffusivity in sponge cake. In their study, a cylinder of sponge cake was put in contact with a high moisture content compartment (agar gel). This

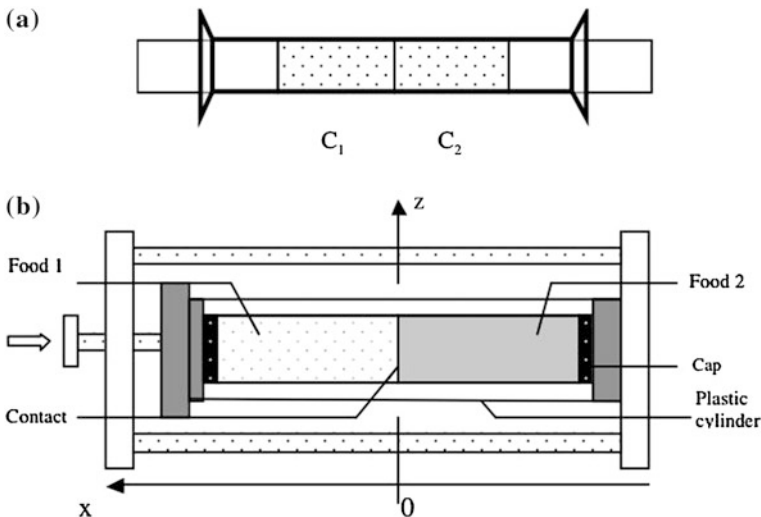


**Fig. 6** Different experimental systems ‘two-phases in contact » permitting one to obtain experiment data for diffusivity identification : (a) system based on two syringes used by Motarjemi (1988) to measure distribution profiles in meat, (b) system of Rougier (2007)

approach was also used by Boudhrioua et al. (2003) to estimate water diffusivity in gelatin–starch gels and by Roca et al. (2006) in a cereal-based product.

However, the moisture loss during slicing of material due to diffusion or evaporation could lead to nonnegligible errors. To avoid diffusion during slicing, Litchfield and Okos (1992) have sliced frozen spaghetti. It is also practically difficult to obtain slices strictly perpendicular to the moisture transfer and, consequently, to have a good repeatability. And finally, the major problem of this technique is to be definitively invasive and destructive and, thus, time consuming. Therefore, several authors have tried to use a noninvasive methodology, such as magnetic resonance imaging (MRI), to obtain a local distribution profile.

MRI is an established technique for non-invasive measurements of moisture and moisture migration in food systems. Conventional MRI techniques are able to produce moisture maps in a very small parallelepiped volume of about  $1 \text{ mm}^3$  with a high degree of resolution. Up to now, MRI has been extensively used in the medical field and has recently been paid more attention as a research tool for studying the drying or rehydration kinetics of food products (Ziegler et al. 2003; Wang et al. 2000; Ruiz-Cabrera 1999; Chen et al. 1997; Schrader and Litchfield 1992). For example, Wang et al. (2000) used MRI to monitor the change in water content in bread/barbeque-chicken bilayer or bread/cheese sandwich systems. Hwang et al. (2009) applied MRI to examine water distribution and migration in rice kernels.

Another nondestructive method consists of measuring the absorption of gamma radiation going through a material. The absorption rate can be related to the moisture content of the sample part passed through by the radiation (Chiang and Petersen 1987).

## ***Factors Affecting the Moisture Diffusivity Values***

The main external parameters controlling the rate of water diffusion are temperature (Arrhenius relationship) and RH. Internal parameters modulating water diffusion are the structure of the food product and, particularly, the porous structure, which induces gaseous diffusion, on the one hand, and the local viscosity of the adsorbed aqueous phase, which, on the other hand, impacts liquid phase diffusion. Variations of apparent water diffusivity resulting from modifications of these parameters (temperature, moisture content, and/or porosity) have been reported for a large range of products.

### ***a. Diffusivity Sensitivity to Moisture Content***

The sensitivity of effective diffusivity ( $D_{\text{eff}}$ ) to RH and, thus, water content is well documented and widely accepted. Figure 7 shows this relation for a variety of food components. Numerous studies have shown that effective diffusivity varied with moisture content, such as, for example, in agar gels (Biquet and Guilbert 1986), in corn-based extruded pasta (Andrieu et al. 1988), in bread, biscuits, and muffins (Tong and Lund 1990), and in sponge cake (Guillard et al. 2003a). Contrary to the

typical  $D_{\text{eff}}$  increase usually observed as a function of moisture content, Karathanos et al. (1990) and Marousis et al. (1989) reported that, in porous starch mixtures,  $D_{\text{eff}}$  can increase with moisture content up to a limit value of 10 % (dry basis) and, then, decrease with moisture content and eventually becomes constant at sufficiently high moistures. This bell-like curve for  $D_{\text{eff}}$  versus moisture content or water activity has recently been observed in hydrophilic materials such as wheat gluten (Angellier-Coussy et al. 2011), starch (Chivrac et al. 2010) or sponge cake and other dry biscuits (Guillard et al. 2003c; Guillard et al. 2004b) (see Fig. 7). This particular behavior was related to change in the structure of the material.

Concerning these structural evolutions with  $a_w$  and their impacts on  $D_{\text{eff}}$ , three kinds of products can be distinguished:

- *Dense, hydrophilic products*, such as starch or wheat gluten edible films. In these materials  $D_{\text{eff}}$  first remained low until an  $a_w$  of 0.4, then it increased up to an  $a_w$  of 0.7–0.8, and finally decreased (Fig. 7). The low and constant  $D_{\text{eff}}$  value obtained for  $a_w < 0.4$ , followed by an increase in  $D_{\text{eff}}$  for  $0.4 < a_w < 0.7$ –0.8, could be related to changes in the mobility of polymer chains (glass transition) due to the plasticizing effect of water. In the high  $a_w$  range, the decrease of the apparent diffusivity in the rubbery wheat gluten film is attributed to a water clustering phenomenon, which would lead to an immobilization of sorbed water molecules and an apparent slower water movement (Gouanve et al. 2007). A decrease in  $D_{\text{eff}}$  with increasing moisture content was also observed in HPMC films by Bilbao-Sainz et al. (2011). They also interpreted the decrease in  $D_{\text{eff}}$  as a clustering of water subsequent to the increase in

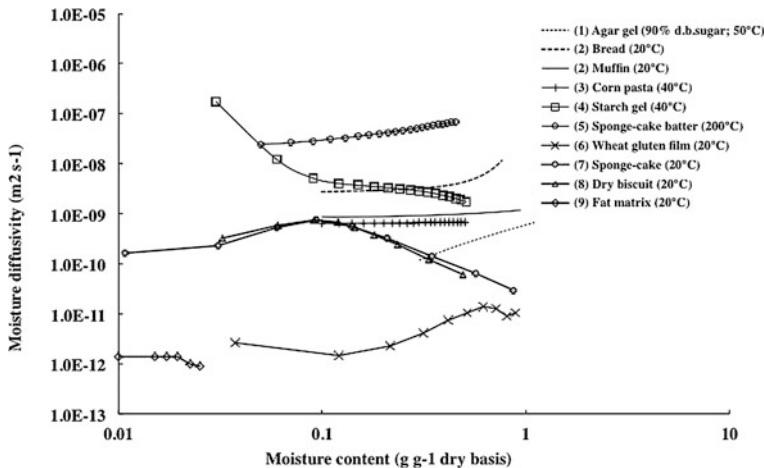


**Fig. 7** Diffusivity of water as a function of moisture content in some food materials. (1) Biquet and Guilbert (1986), (2) Tong and Lund (1990), (3) Andrieu et al. (1988), (4) Marousis et al. (1991), (5) Baik and Marcotte (2003), (6) Angellier-Coussy et al. (2011), (7) Guillard et al. (2003a); (8) Guillard et al. (2004b) and (9) Bourlieu et al. (2006)

water content resulting in “free water.” These free molecules, without interaction with the matrix, aggregate to form di-, tri-, and tetra-mer clusters. These clusters present higher molecular volume than do monomers; thus, they diffuse more slowly and induce a drop in  $D_{\text{eff}}$ .

- *Porous products*, such as sponge cake. In these materials, through water adsorption, the matrix swells, leading to a decrease in the porosity of the product. As a consequence, water liquid diffusion in the solid matrix would predominate at this stage, as compared with the water vapor diffusion in the open pores. Since liquid diffusion of water (about  $10^{-9} \text{ m}^2/\text{s}^1$ ) is slower than vapor diffusion of water (about  $10^{-5} \text{ m}^2/\text{s}^1$ ), the resulting effective water diffusivity decreased with the increasing moisture content of the sponge cake. This impact of swelling and decrease in porosity was pointed out by Environmental SEM by Guillard et al. (2003c) (see Fig. 8). Through water adsorption in sponge cake, a swollen matrix was formed, and the apparent degree of porosity decreased strongly near saturation, leading to a predominant water liquid diffusion. Then, near saturation, water diffusivity of the sponge cake was quite constant, because most of the porous structure had collapsed, and water transport occurred mainly in the liquid phase within the swollen matrix.
- Conversely, in *dense highly hydrophobic* materials, such as lipid-based edible barrier films (such as WAX/ACETOGLYCERIDES composite materials), sorbing a very small amount of water (GAB parameters of  $Q_{\text{mono}} = 0.0085$ ,  $C = 1.2351$ ,  $K = 0.7893$ ), a quasi-constant  $D_{\text{eff}}$  ( $\sim 0.05 \times 10^{10} \text{ m}^2 \text{ s}^{-1}$ ) was reported (Bourlieu et al. 2008). This low  $D_{\text{eff}}$  was coherent with the hydrophobic partially crystalline nature of the material (solid fat content of 88 % at the temperature considered). At high  $a_w$ , the sorption of water did not plasticize this inert matrix or modify its barrier properties.

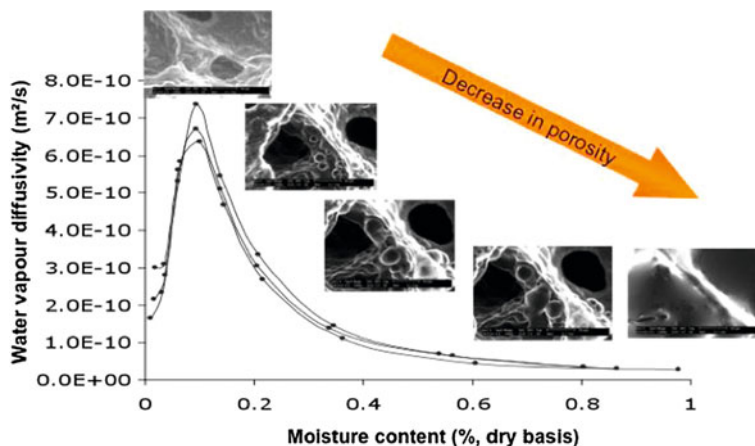


**Fig. 8** Evolution of water vapour diffusivity in sponge cake as a function of moisture content and subsequent change in porosity as observed by ESEM—adapted from Guillard et al. (2003a, d)

It is clear from these results that structural parameters (e.g., porosity change, glass transition, etc.) are more relevant parameters for describing water diffusivity change in food and nonfood products than is an increase or decrease in product moisture content. Nevertheless, up to now, the variations of water diffusivity were scarcely quantitatively related to structural changes, and the classical relationship  $D_{\text{eff}} = f(Q_w)$  is still used in food science.

### *b. Typical Values of Water Vapor Diffusivity in Foodstuffs*

According to the various structures of food matrices, typical values of effective diffusivity varied from  $1 \times 10^{-9}$  to  $1 \times 10^{-12} \text{ m}^2 \text{ s}^{-1}$ , with higher values for porous products such as cereal-based foods (Guillard et al. 2003a) and lower values for dense materials such as raisins or dates (Gencturk et al. 1986; Tütüncü and Labuza 1996) (Fig. 9). Extreme range of values of diffusion reported for the sake of comparison reaches  $2.4 \times 10^{-5} \text{ m}^2 \text{ s}^{-1}$  for water vapor in air, whereas self-diffusion coefficient of liquid water is  $2 \times 10^{-9} \text{ m}^2 \text{ s}^{-1}$  and lower limits reported in glassy materials average  $2 \times 10^{-14} \text{ m}^2 \text{ s}^{-1}$  (Gekas 1992). Moisture diffusivity is very sensitive to the variations in composition and structure of the examined materials. But even for the same food material, variations in diffusivity values are generally encountered between two investigations, proving that diffusivity is also very sensitive to the particular experimental and mathematical methods used for its determination.

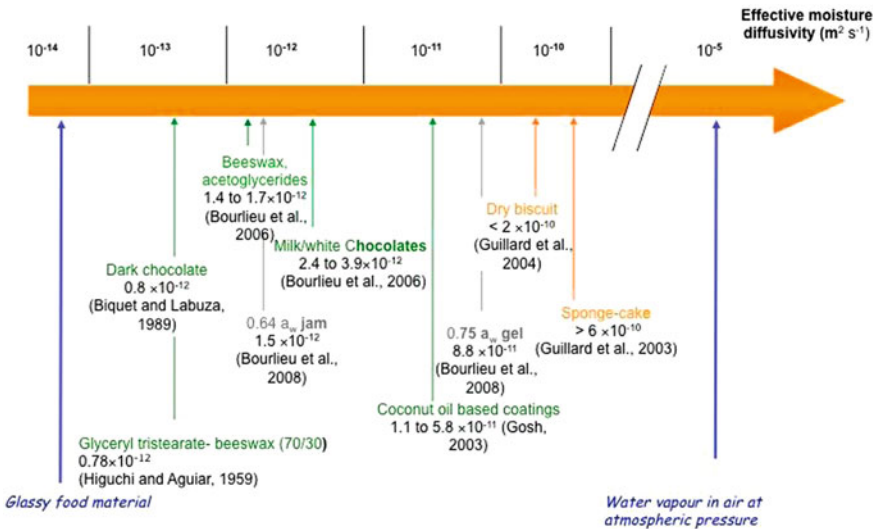


**Fig. 9** Range of values for water vapour diffusivity in foodstuffs and edible coatings (data from Biquet and Labuza 1988; Bourlieu et al. 2006, 2008; Ghosh 2003; Guillard et al. 2003, 2004; Higuchi and Aguiar 1959)



### *c. Validity and Accuracy of Identified Diffusivity Values*

No standard method of diffusivity estimation exists. As regards to the economical importance of drying, many investigators have been interested in modeling drying kinetics in order to optimize processes and, thus, have determined moisture diffusivity in food matrices subject to drying. Whatever the experimental method used, the same analytical treatment of experimental data is usually performed. Moisture diffusivity is identified by minimizing error between experimental and predicted moisture contents obtained by experimental monitoring of mass change during drying, desorption, or sorption experiment. When  $D_{\text{eff}}$  is suspected to vary with moisture content, which is almost always verified, a diffusivity law as a function of moisture content is chosen a priori, and the parameters of this law are identified in the same manner as the constant value.

Zogzas et al. (1996) reviewed the different  $D_{\text{eff}}$  laws as a function of moisture content encountered in the literature. Contrary to  $D_{\text{eff}}$  variations with temperature, which are almost always represented through an Arrhenius equation, diffusivity dependence on moisture content, whose variety of behaviors have been previously displayed in Fig. 7, has been represented by various empirical relations relying on numerous parameters (from 3 to 5) (Table 3).

More complex relations are provided when simultaneous temperature and moisture content, but also porosity, dependence of  $D_{\text{eff}}$  is taken into account as listed in Table 3. From this complexity of relations but, also, of methods used for generating experimental data and mathematical solutions chosen for analytical treatment of data, large variations in  $D_{\text{eff}}$  values are observed even for the same material, such as in corn, where it was found that  $D_{\text{eff}}$  varied from  $5 \times 10^{-12}$  to  $8 \times 10^{-7} \text{ m}^2 \text{ s}^{-1}$  for the same moisture content range.

## ***Water Vapor Permeability***

The water vapor permeability (WVP) of a film is a steady state property that describes the rate of water transfer through the film and summarizes the phase of adsorption, water vapor diffusion in the film matrix, and desorption on the other side of the film. This rate is obtained for a given RH difference, which is applied on each side of the film usually using a permeation cell that contains a desiccant or saturated solution and is stored in a desiccator at a given RH and is hermetically sealed with the barrier film (American ASTM E96-80; ASTM 1980). Comprehensive tables of WVP values have recently been proposed by Morillon et al. (2002), Wu et al. (2002), and Bourlieu et al. (2009b). Examples of values taken from Bourlieu et al. (2009) summarize the range of moisture WVP values encountered in food coating, in comparison with polymeric packaging, at 20 °C are presented in Table 4.

**Table 3** Empirical parametric models expressing diffusivity as a function of temperature and moisture content for various food materials (X g/g, T degree K)

Num. of par	Material	Parametric model	Reference
2	Swordfish	$D(X) = a_0 + a_1 X$ $a_0 = 9 \times 10^{-11}$ , $a_1 = 1.6 \times 10^{-10}$ $1.0 \leq X \leq 5.0$ , $313 \leq T \leq 328$	Del Valle and Nickerson (1968)
	Cereals	$a_0 = 1.35 \times 10^{-2}$ , $a_1 = 4.2 \times 10^{-4}$ $0.1 \leq X \leq 0.3$ , $T = 330$	Whitaker et al. (1969)
	Sponge cake	$D(X) = D_0 X^\alpha$ $D_0 = 2.3 \times 10^{-11}$ , $\alpha = -1.6$ $0.20 \leq X \leq 0.70$ (wet basis), $T = 293$	Guillard et al. (2003c)
3	Corn	$D(X, t) = a_0 \exp(a_1 X) \exp(-\frac{a_2}{T})$ $a_0 = 7.817 \times 10^{-5}$ (or $4.067 \times 10^{-5}$ ), $a_1 = 5.5$ , $a_2 = 4850$ $0.05 \leq X \leq 0.4$ , $283 \leq T \leq 300$	Parti and Dugmanics (1990)
	Carrot	$a_0 = 1.053 \times 10^{-4}$ , $a_1 = 0.059$ , $a_2 = 3460$ $0.0 \leq X \leq 5.0$ , $303 \leq T \leq 343$	Mulet (1994)
	Starch (granular)	$a_0 = 5.321 \times 10^{-6}$ , $a_1 = -1.511$ , $a_2 = 2848.5$ $0.11 \leq X \leq 0.5$ , $298 \leq T \leq 413$ at 1 atm pressure	Karathanos et al. (1994)
	Onion	$D(X, T) = a_0 \exp(-\frac{a_1}{X}) \exp(-\frac{a_2}{T})$ $a_0 = 3.72$ , $a_1 = 8.63 \times 10^{-2}$ , $a_2 = 7110$ $0.05 \leq X \leq 18.7$ , $333 \leq T \leq 353$	Kiranoudis et al. (1992)
	Potato	$a_0 = 1.29 \times 10^{-6}$ , $a_1 = 7.25 \times 10^{-2}$ , $a_2 = 2044$ $0.03 \leq X \leq 5.0$ , $333 \leq T \leq 373$	Kiranoudis et al. (1995)
	Carrot	$a_0 = 2.71 \times 10^{-7}$ , $a_1 = 7.44 \times 10^{-2}$ , $a_2 = 1527$ $0.03 \leq X \leq 5.0$ , $333 \leq T \leq 373$	Kiranoudis et al. (1995)
	Starch gel (amioca)	$D(X, T) = a_0 [1 - \exp(-a_1 X)] \exp(-\frac{a_2}{T})$ $a_0 = 4.8 \times 10^{-6}$ , $a_1 = 2.8$ , $a_2 = 3668.4$ ; $0.01 \leq X \leq 1.0$ , $T = 333$ $a_0 = 4.8 \times 10^{-6}$ , $a_1 = 0.9$ , $a_2 = 3668.4$ ; $0.01 \leq X \leq 1.0$ , $T = 373$	Vagenas and Karathanos (1993)
	Starch gel	$D(X, T) = (a_0 + a_1 T) \left( \frac{X_0}{1+X_0} - \frac{X}{1+X} \right)^{a_2}$ $a_0 = 12.96 \times 10^{-11}$ , $a_1 = 2.72 \times 10^{-11}$ , $a_2 = 0.02$ $0.2 \leq X \leq 1.7$ , $303 \leq T \leq 323$ , pressure: $P = 1$ bar	Buvanasundaram et al. (1994)
	Baking cake	$D(X, T) = a_0 \exp[-\frac{a_1}{T} + a_2 X]$ $a_0 = 9.75$ , $a_1 = 7689.9$ , $a_2 = -0.0858$ $0.369 \leq X \leq 0.707$ , $306 \leq T \leq 395$	Baik and Marcotte (2002)
	Pasta (corn)	$D(X, T) = (a_0 + a_1 X + a_2 X^2) \exp(-\frac{a_3}{T})$ $a_0 = 1.15 \times 10^{-3}$ , $a_1 = 1.67 \times 10^{-2}$ , $a_2 = 7.8 \times 10^{-2}$ , $a_3 = 5840$ $0.1 \leq X \leq 0.5$ , $313 \leq T \leq 353$	Andrieu et al. (1988)

(continued)

**Table 3** (continued)

Num. of par	Material	Parametric model	Reference
	Apple	$D(X, T) = a_0 \exp(a_1 X) \exp\left(-\frac{a_2 X + a_3}{T}\right)$ $a_0 = 2.75 \times 10^{-3}$ , $a_1 = 12.97$ , $a_2 = 4216$ , $a_3 = 5267$ $0.04 \leq X \leq 1.3$ , $288 \leq T \leq 318$	Singh et al. (1984)
	Corn (shelled)	$D(X, T) = a_0 \exp[(a_1 T - a_2)X] \exp\left(-\frac{a_3}{T}\right)$ $a_0 = 4.254 \times 10^{-8}$ , $a_1 = 4.5 \times 10^{-2}$ , $a_2 = 5.5$ , $a_3 = 2513$ $0.05 \leq X \leq 0.35$ , $323 \leq T \leq 343$	Chu and Hustrulid (1968)
	Corn	$a_0 = 2.54 \times 10^{-8}$ , $a_1 = 1.2343 \times 10^{-1}$ , $a_2 = 45.47$ , $a_3 = 1183.3$ $0.1 \leq X \leq 0.4$ , $293 \leq T \leq 338$	Ulku and Uckan (1986)
	Corn	$a_0 = 1.905 \times 10^{-5} X_0$ , $a_1 = 1.83 \times 10^{-2}$ , $a_2 = 2.37$ , $a_3 = 2153$ $0.1 \leq X \leq 0.45$ , $323 \leq T \leq 393$	Mourad et al. (1994)
	Rice	$a_0 = 2.744 \times 10^{-6}$ , $a_1 = 1.589 \times 10^{-3}$ , $a_2 = 0.379$ , $a_3 = 4294.8$ $0.26 \leq X \leq 0.32$ , $321.8 \leq T \leq 355.2$	
5		$D(X, T) = a_0 \exp\left(\sum_{i=1}^3 a_i X^i\right) \exp\left(-\frac{a_4}{T}\right)$	
	Bread	$a_0 = 2.8945$ , $a_1 = 1.26$ , $a_2 = -2.76$ , $a_3 = 4.96$ , $a_4 = 6117.4$ $0.1 \leq X \leq 0.75$ , $293 \leq T \leq 373$	Tong and Lund (1990)
	Biscuit	$a_0 = 0.92114$ , $a_1 = 0.45$ , $a_2 = 0$ , $a_3 = 0$ , $a_4 = 6104.5$ $0.1 \leq X \leq 0.6$ , $293 \leq T \leq 373$	Tong and Lund (1990)
	Muffin	$a_0 = 6.16729$ , $a_1 = 0.39$ , $a_2 = 0$ , $a_3 = 0$ , $a_4 = 6664.0$ $0.1 \leq X \leq 0.95$ , $293 \leq T \leq 373$	Tong and Lund (1990)
		$D(X) = D_0 \sum_{i=1}^n \alpha_i X^i$	
	Dry biscuit	$D_0 = 3.06 \times 10^{-10}$ , $a_1 = -628.30$ , $a_2 = 733.33$ , $a_3 = -287.94$ , $a_4 = 36.96$ $0 \leq X \leq 0.30$ (wet basis), $T = 293$	Guillard et al. (2004b)
	Pasta (dur. semolina)	$D(X, T) = a_0 [1 - \exp(-a_1 X^{a_2}) + X^{a_3}] \exp\left(-\frac{a_4}{T}\right)$ $a_0 = 2.392 \times 10^{-7}$ , $a_1 = 7.9082 \times 10^{-14}$ , $a_2 = 15.7$ , $a_3 = 0.6859$ , $a_4 = 3156.3$ $0.015 \leq X \leq 0.26$ , $313 \leq T \leq 353$	Litchfield and Okos (1992)
	Starch gel	$D(X, T) = \left[a_0 + a_1 X^{-a_2} + a_3 \frac{\varepsilon^3}{(1-\varepsilon)^2}\right] \exp\left(-\frac{a_4}{T}\right)$ $a_0 = 4.84 \times 10^{-7}$ , $a_1 = 5.735 \times 10^{-11}$ , $a_2 = 4.337$ , $a_3 = 3.42 \times 10^{-6}$ , $a_4 = 2264$ $0.03 \leq X \leq 0.5$ , $313 \leq T \leq 373$ , pressure : $P = 1$ bar $\varepsilon = (0.6 + 0.0643X$ $-0.37X^2) \exp(0.0077 - 0.113X \times P)$	Marousis et al. (1991)

**Table 4** Comparison of moisture water vapor permeability (WVP; 20 °C) ranges for edible coatings in comparison with most commonly used synthetic packaging films

Film or coating	WVP ( $10^{-11}$ g m $^{-1}$ s $^{-1}$ Pa $^{-1}$ )	RH difference (%)	Thickness (mm)	Temperature (°C)	Reference
<i>Synthetic films</i>					
Aluminium	0.0005	0–98	(–)	38	(Myers et al. 1961)
HPDE	0.002	0–100	0.019	27.6	(Shellhammer et al. 1997)
PP	0.010		0.025	25	
PVC	0.041		0.012	27.6	
Lipid films	0.03–1.0	0–100		20	
<i>Waxes</i>					
Candelilla wax	0.014	0–100	0.14	24.9	(Shellhammer et al. 1997)
Paraffin	0.023		0.66	25	(Lovegren and Feuge 1954)
Beeswax	0.103		0.14	25.9	(Shellhammer et al. 1997)
Carnauba wax	0.114		0.130	27.5	
<i>Fatty acids</i>					
Capric acid	0.38	12–56			(Koelsch and Labuza 1992)
Palmitic acid	0.65				
Stearic acid	0.22				
<i>Triglycerides &amp; derivatives</i>					
Tripalmitin	0.225	0–100	0.130	27.5	(Shellhammer and Krochta 1997a)
Triolein	12.100	22.84		25	(Quezada Gallo 1999)
Anhydrous milkfat	1.028	0–100	0.130	24.9	(Shellhammer et al. 1997)
Hydrogenated peanut oil	3.863		3.39	25	(Lovegren and Feuge 1954)
Glyceryl monostearate	0.77		1.026	24.3	(Higuchi and Aguiar 1959)
Acetomonopalmitine	11.35		0.200	20	(Bourlieu et al. 2006)
Tempered cocoa butter	26.8–61.2		1.59–2.92	26.7	(Landmann et al. 1960)
Milk chocolate	88.99		0.68	20	(Bourlieu et al. 2006)
<i>Protein films</i>	1.0–100.0	0–100		20	

(continued)

Table 4 (continued)

Film or coating	WVP( $10^{-11}$ g m $^{-1}$ s $^{-1}$ Pa $^{-1}$ )	RH difference (%)	Thickness(mm)	Temperature (°C)
Reference	Wheat Gluten	12.97	0.053	20
(Guillard et al. 2003a)				
Soya	281.18	50-66	0.072	25 (Rhim et al. 2002)
Com zein	11.6	0-85	0.12-0.33	21 (Park and Chinnan 1995)
<i>Polysaccharide films</i>	1.0-10.0	0-100	20	
Cellulose derivatives	9.2-11.0	0-85	0.04-0.07	21 (Park and Chinnan 1995)
Starch	25-78	11-100	0.005-0.180	30 (Bertuzzi et al.)

From a theoretical point of view, the WVP through a barrier is determined combining Fick's first law of diffusion (Eq. 7) with Henry's law of solubility (Eq. 10) as expressed in Eq. 11 (Park 1986; ASTM 1980):

$$Q = S \cdot p \quad (10)$$

where  $Q$  is the concentration of the permeate ( $\text{mol m}^{-3}$ ),  $S$  the solubility coefficient defined as the maximum mass of the migrating molecule that dissolves in a unit volume of the material at equilibrium ( $\text{mol m}^{-3} \text{ Pa}^{-1}$ ), and  $p$  the permeate partial pressure in the adjacent air (Pa):

$$\text{WVP} = D_{\text{eff}} \cdot S = \frac{J \cdot e}{A \cdot \Delta p \cdot M} \quad (11)$$

where WVP is the water vapor permeability ( $\text{mol m}^{-1} \text{ s}^{-1} \text{ Pa}^{-1}$ ),  $A$  the surface of barrier ( $\text{m}^2$ ),  $M$  the water molar weight ( $\text{g mol}^{-1}$ ), and  $e$  (m) the barrier thickness.

As is expressed in Eq. 11, WVP is the resultant of two parameters: a thermodynamic parameter, solubility, which depends on the compatibility between the penetrant molecule at equilibrium and the material the penetrant is migrating through, and a nonthermodynamic kinetic parameter  $D_{\text{eff}}$ , indicating water mobility in the material and highly influenced by the structural and morphological characteristics of the material. The range of validity of Eq. 11 is limited to thin, nonporous, hydrophobic film, with low water vapor solubility, nonswelling, and constant permeation rate over time, whereas in most other cases (hydrophilic material that interacts with water), a given value of WVP cannot be considered as an inherent property of the film, since its value will be influenced by extrinsic parameters of the WVP test such as the difference of RH, the temperature of the test, and the thickness of the barrier (McHugh et al. 1993; McHugh and Krochta 1994; Morillon et al. 2002).

The WVP is often preferred over diffusivity value to characterize the moisture barrier property of edible films and coatings. Even if this parameter represents an overall moisture transport mixing both sorption and diffusion phenomena, it is convenient to classify and compare the ability of edible films to prevent moisture loss or gain when applied directly onto a food surface or when used at the interface between two food compartments of contrasted initial water activities. In the last case, the edible film aims at preventing moisture exchange between the high  $a_w$  compartment to the one with a lower  $a_w$ . Usually, the low  $a_w$  compartment is a cereal-based compartment such as, for example, a crispy biscuit or wafer (Guillard et al. 2004a; Bourlieu et al. 2006) associated to a moist filling such as jam, pastry cream, and so forth. Edible barrier films, almost always lipid-based films, are very interesting solutions to slow down moisture transfer between food compartments and to increase the shelf life of the overall product, limiting texture loss (Roca et al. 2008).

However, WVP is usually measured for a given RH difference, often 0–100 % RH, which is rarely representative of the conditions that prevail in multicompartment foods. For example, classical association of a crispy wafer with a jam

provided a difference of  $a_w$  around 0.14–0.50 (Bourlieu et al. 2006) or of a sponge cake with a moist filling an  $a_w$  difference of 0.84–0.95 (Guillard et al. 2003a). If WVP remains quite constant on the entire RH range for pure hydrophobic films, it is not the case for materials containing hydrophilic components. A typical example of such material very often used in food industry as edible film and coating is chocolate. For an  $a_w > 0.80$ , sugar particles contained in the continuous fat layer of chocolate begin to sorb a lot of water, to dissolve, and to swell. This is revealed by a sharp increase of the sorption isotherm curve of chocolate (Guillard et al. 2003d) and a nonlinearity of WVP evolution with RH difference for RH above 80 %. Consequently, if chocolate layers are good moisture barrier coating a low  $a_w$  (below 0.80), they are definitively inefficient for high  $a_w$ . Therefore, to be more predictive of the moisture barrier efficiency, some authors (Guillard et al. 2003d; Bourlieu et al. 2006) have used diffusivity coefficient and water vapor sorption isotherm instead of WVP as input parameters in Fick's second law for predicting moisture transfer through edible film placed at the interface between two domains of a composite food. They demonstrated that this approach was much more accurate in classifying moisture barrier efficiency of edible films and coatings.

Food Structure and Moisture Transfer

A Modeling Approach

Guillard, V.; Bourlieu, C.; Gontard, N.

2013, VII, 60 p. 13 illus., 6 illus. in color., Softcover

ISBN: 978-1-4614-6341-2